PHYSICAL REVIEW D **93,** 035007 (2016)

Search for mirror quarks at the LHC

Shreyashi Chakdar,[1,2,*] K. Ghosh,[1,†] V. Hoang,[2,‡] P. Q. Hung,[2,3,§] and S. Nandi[1,‖]

[1]*Department of Physics and Oklahoma Center for High Energy Physics, Oklahoma State University, Stillwater, Oklahoma 74078-3072, USA*

[2]*Department of Physics, University of Virginia, Charlottesville, Virginia 22904-4714, USA*

[3]*Center for Theoretical and Computational Physics, Hue University College of Education, Hue, Vietnam*

(Received 25 September 2015; published 5 February 2016)

Observation of nonzero neutrino masses at a scale $\sim 10^{-1}$–10^{-2} eV is a major problem in the otherwise highly successful Standard Model. The most elegant mechanism to explain such tiny neutrino masses is the seesaw mechanism with right-handed neutrinos. However, the required seesaw scale is so high, $\sim 10^{14}$ GeV, it will not have any collider implications. Recently, an explicit model has been constructed to realize the seesaw mechanism with the right-handed neutrinos at the electroweak scale. The model has a mirror symmetry, having both the left and right lepton and quark doublets and singlets for the same $SU(2)_W$ gauge symmetry. Additional Higgs multiplets have been introduced to realize this scenario. It turns out that these extra Higgs fields also help to satisfy the precision electroweak tests, and other observables. Because the scale of the symmetry breaking is electroweak, both the mirror quark and the mirror leptons have masses in the electroweak scale in the range ~150–800 GeV. The mirror quarks/leptons decay to ordinary quarks/leptons plus very light neutral scalars. In this work, we calculate the final-state signals arising from the pair productions of these mirror quarks and their subsequent decays. We find that these signals are well observable over the Standard Model background for the 13 TeV LHC. Depending on the associated Yukawa couplings, these decays can also give rise to displaced vertices with long decay lengths, very different from the usual displaced vertices associated with b decays.

DOI: 10.1103/PhysRevD.93.035007

I. INTRODUCTION

Two of the outstanding experimental problems of the highly successful Standard Model (SM) are the existence of nonzero neutrino masses and dark matter. One can obtain nonzero neutrino masses in the SM from the effective dimension 5 operators [1] (such as the Weinberg operator, having the schematic structure of LLHH, where L is a lepton doublet and H the Higgs doublet), but if the Planck scale is the next scale in the theory beyond the TeV scale, then the neutrino masses come out a few orders of magnitude smaller compared to the observed values. The scale needed is $\sim 10^{14}$ GeV. If there are right-handed (RH) SM singlet neutrinos at this scale, then such effective operators can be obtained by integrating out the heavy RH neutrinos. A seesaw mechanism constructed by postulating such SM singlet RH neutrinos is the most elegant mechanism to explain these tiny neutrino masses. However, the existence of such a heavy RH singlet neutrino cannot be tested in any laboratory experiments, especially in the currently running high-energy large hadron colliders (LHCs). Also, fermion representation in the SM is very asymmetric; left-handed (LH) fermions are doublets, whereas RH fermions are singlets. Long ago, it was proposed that maybe nature is more symmetric; there are similar heavy particles with exactly opposite chirality [2]. However, such a simple extension is excluded by the currently available precision electroweak data, namely the S parameter. Recently, a new mirror symmetric model has been proposed [3] which rectifies the old Lee-Yang proposal by extending the Higgs sector. The electroweak gauge symmetry is $SU(2)_W \times U(1)_Y$, and for every left-handed SM doublet, there are right-handed SM doublets with new fermions. Similarly, for every RH SM singlet, we have new LH singlet fermions. These new fermions are called mirror fermions. The EW precision constraints, such as the S parameter, are satisfied by extending the Higgs sector to include $SU(2)$ triplet Higgses. The $SU(2)_W \times U(1)_Y$ symmetry is broken in the same electroweak scale, $\Lambda_{\rm EW} \sim 246$ GeV. All the particles get masses from the spontaneous symmetry breaking in this scale and will have masses less than a TeV. Notice also the marked difference from the left-right (L-R) symmetric model [4], which is characterized by an extra $SU(2)_R$ with right-handed fermions transforming as doublets under that new gauge group. Furthermore, the L-R model contains *two* symmetry breaking scales, Λ_L and Λ_R, with the latter being completely arbitrary and constrained experimentally from below by the latest LHC data [5], $M_R \gtrsim 3$ TeV. In the L-R model, the masses of the right-handed neutrinos are proportional to the $SU(2)_R$ scale.

*chakdar@virginia.edu
†kirti.gh@gmail.com
‡vvh9ux@virginia.edu
§pqh@virginia.edu
‖s.nandi@okstate.edu

In this model, the RH neutrinos which are doublet under the $SU(2)$ gauge symmetry will have masses in the electroweak scale. An explicit model was constructed in which a seesaw mechanism is realized to obtain tiny neutrino masses with the RH neutrinos at the EW scale [3]. The implications for the model for neutrino masses and mixings, precision EW tests, and lepton-violating rare processes were discussed in Refs. [6–8]. This model uses an A_4 (Table I, [8]) discrete symmetry. In addition to the usual Higgs doublet, it has a second Higgs doublet, two Higgs triplets, and several Higgs singlets. After the symmetry breaking, the neutral Higgses mix. One of the neutral Higgses is the recently observed 125 GeV Higgs boson. The model also has doubly charged Higgses and singly charged Higgses, as well as additional massive neutral Higgses. A previous analysis of some aspects of this scalar sector can be found in Ref. [9].

In this work, we explore the collider implications of this model. The model has mirror fermions, RH doublets and LH singlets, particularly the mirror quarks. These particles have masses below ~800 GeV to satisfy unitarity, and can be copiously produced at the LHC via their strong color interaction. These can only decay to ordinary quarks and essentially massless scalars. Depending on the relevant Yukawa couplings, these mirror quarks may decay immediately, or may have long life. If they decay immediately, we will get a final state with high-p_T jets, and large missing energy due to the escaping light scalars. If they have long life, then they can give rise to 2-jets which are coming from displaced vertices. Therefore, the final-state signature, in this case, is characterized by 2-jets plus missing transverse momentum ($\not{p}_T$), where the jets are not pointing towards the primary vertex. For the LHC multi-jets + $\not{p}_T$ analysis, such jets are usually considered as "fake jets" not originating from the hard scattering, and thus rejected as beam-induced background and cosmic rays [10,11].

Our presentation below is as follows: In Secs. II through V, we review the model and the formalism, as well as the the constraints from the electroweak precision tests and the Higgs data. Section VI contains our new results, where we discuss the implications of the models at the LHC. We conclude in Sec. VII.

We end this introduction by mentioning an aspect of the SM which often goes unnoticed. The electroweak phase transition is intrinsically nonperturbative, and a common framework for studying nonperturbative phenomena is that of lattice gauge theory. It has been problematic to put a chiral gauge theory such as the SM on the lattice because of the loss of gauge invariance. Reference [12] proposed the introduction of mirror fermions in order to achieve a gauge-invariant formulation of the SM on the lattice. The mirror fermions of the EW-scale ν_R model would play such a role.

Finally, we take the liberty to quote a sentence from the famous paper about parity violation by Lee and Yang [2]: "If such asymmetry is indeed found, the question could still be raised whether there could not exist corresponding elementary particles exhibiting opposite asymmetry such that in the broader sense there will still be overall right-left symmetry." The EW-scale ν_R model [3] is a direct response to this famous quote and is a model which satisfies the electroweak precision data as we have mentioned above.

II. THE MODEL, FORMALISM, AND EXISTING CONSTRAINTS

The EW-scale ν_R model [3] is basically the SM with an extended fermionic (and scalar) sector: For every SM left-handed doublet, there is a mirror right-handed doublet, and for every SM right-handed singlet, there is a mirror left-handed singlet. The gauge group remains the same and, as such, the energy scale characterizing the EW-scale ν_R model is still the electroweak scale $\Lambda_{\rm EW} \sim 246$ GeV. This is the reason, as we shall see in the brief review, for the Majorana mass of the right-handed neutrinos to be bounded from above by the electroweak scale and, as a consequence, for its accessibility at colliders such as the LHC and the International Linear Collider (ILC). However, it is important to note that as discussed in Ref. [7] in detail, the statement that the right-handed neutrino masses are bounded by the electroweak scale is assuming $g_M \sim O(1)$.

(1) *Gauge group of the EW-scale ν_R model:*

$$SU(3)_C \times SU(2)_W \times U(1)_Y. \tag{1}$$

Notice the absence of the subscript "L" in $SU(2)$. This is because the EW-scale ν_R model accommodates both SM fermions and the mirror counterparts of opposite chirality. Notice also the marked difference from the left-right symmetric model [4], which is characterized by an extra $SU(2)_R$, with right-handed fermions transforming as doublets under that new gauge group. Furthermore, the L-R model contains *two* symmetry-breaking scales Λ_L and Λ_R, with the latter being completely arbitrary and constrained experimentally from below by the latest LHC data [5], $M_R \gtrsim 3$ TeV. In the L-R model, the masses of the right-handed neutrinos are proportional to the $SU(2)_R$ scale.

(2) *Fermion $SU(2)_W$ doublets* (M refers to mirror fermions):

$$\text{SM: } l_L = \begin{pmatrix} \nu_L \\ e_L \end{pmatrix}, \text{ Mirror: } l_R^M = \begin{pmatrix} \nu_R^M \\ e_R^M \end{pmatrix},$$

$$\text{SM: } q_L = \begin{pmatrix} u_L \\ d_L \end{pmatrix}, \text{ Mirror: } q_R^M = \begin{pmatrix} u_R^M \\ d_R^M \end{pmatrix}.$$

(3) *Fermion $SU(2)_W$ singlets*:

$$\text{SM: } e_R; u_R, d_R. \text{ Mirror: } e_L^M; u_L^M, d_L^M.$$

(4) *Scalar sector:*

(a) A singlet scalar Higgs ϕ_S with $\langle\phi_S\rangle = v_S$. In Ref. [3], it was stated that the Dirac mass appearing in the seesaw formula, namely $m_\nu^D = g_{Sl} v_S$ (see the review below), has to be less than 100 keV in order for $m_\nu < O(\text{eV})$, because $M \sim O(\Lambda_{\text{EW}})$. Furthermore, if one assumes $g_{Sl} \sim O(1)$, then $v_S \sim O(100\ \text{keV})$, and the Higgs singlet particle mass will be comparable to that value or smaller, and will be much lighter than the other particles. However, an updated analysis of $\mu \to e\gamma$ [13] constrains $g_{Sl} < 10^{-3}$, which gives $v_S \sim O(100\ \text{MeV})$. Nevertheless, one can easily constrain the mass of the physical Higgs singlet scalar to be smaller than that value. In what follows, we could safely ignore the singlet mass in our phenomenological analysis. Notice that the aforementioned statements are independent of the values of the Yukawa couplings g_{Sq} present in the SM mirror-singlet Higgs interactions which are not constrained by experiment at this moment.

(b) Doublet Higgses:

$$\Phi_2 = \begin{pmatrix} \phi_2^+ \\ \phi_2^0 \end{pmatrix} \text{ with } \langle\phi_2^0\rangle = v_2/\sqrt{2}.$$

In the original version [3], this Higgs doublet couples to both SM and mirror fermions. An extended version was proposed [7] in order to accommodate the 125 GeV SM-like scalar and, in this version, Φ_2 only couples to SM fermions, while another doublet Φ_{2M}, whose vacuum expectation value (VEV) is $\langle\phi_{2M}^0\rangle = v_{2M}/\sqrt{2}$, couples only to mirror fermions.

(c) Higgs triplets:

(i) $\tilde{\chi}(Y/2=1) = \frac{1}{\sqrt{2}}\vec{\tau}.\vec{\chi} = \begin{pmatrix} \frac{1}{\sqrt{2}}\chi^+ & \chi^{++} \\ \chi^0 & -\frac{1}{\sqrt{2}}\chi^+ \end{pmatrix}$, with $\langle\chi^0\rangle = v_M$.

(ii) $\xi(Y/2=0)$ in order to restore custodial symmetry, with $\langle\xi^0\rangle = v_M$.

(iii) VEVs:

$$v_2^2 + v_{2M}^2 + 8v_M^2 = v^2 \approx (246\ \text{GeV})^2$$

(5) *Dirac and Majorana neutrino masses*: For simplicity, from hereon, we will write ν_R^M simply as ν_R.

(i) Dirac neutrino mass:

The singlet scalar field ϕ_S couples to a fermion bilinearly

$$\begin{aligned} L_S &= g_{Sl}\bar{l}_L\phi_S l_R^M + \text{H.c.} \\ &= g_{Sl}(\bar{\nu}_L\nu_R + \bar{e}_L e_R^M)\phi_S + \text{H.c.} \end{aligned} \quad (2)$$

From (2), we get the Dirac neutrino masses $m_\nu^D = g_{Sl} v_S$.

(ii) Majorana neutrino mass:

$$\begin{aligned} L_M &= g_M l_R^{M,T}\sigma_2\tau_2\tilde{\chi} l_R^M \\ &= g_M \nu_R^T\sigma_2\nu_R\chi^0 - \frac{1}{\sqrt{2}}\nu_R^T\sigma_2 e_R^M\chi^+ \\ &\quad - \frac{1}{\sqrt{2}} e_R^{M,T}\sigma_2\nu_R\chi^+ + e_R^{M,T}\sigma_2 e_R^M\chi^{++}. \end{aligned} \quad (3)$$

From (3), we obtain the Majorana mass $M_R = g_M v_M$.

It is important to note here that in the original version [3], a global symmetry denoted by $U(1)_M$ was assumed under which the mirror right-handed doublets and left-handed singlets transform as $(l_R^M, e_L^M) \to e^{\imath\theta_M}(l_R^M, e_L^M)$ and the triplet and singlet Higgs fields transform as $\tilde{\chi} \to e^{-2\imath\theta_M}\tilde{\chi}$, $\phi_S \to e^{-\imath\theta_M}\phi_S$, with all other fields being singlets under $U(1)_M$. With this transformation, a coupling similar to Eq. (3) is forbidden for the SM leptons, and hence there is no Majorana mass for left-handed neutrinos at tree level. It was also shown in Ref. [3] that the Majorana mass for left-handed neutrinos can arise at one loop but is much smaller than the light neutrino mass and thus can be ignored.

The next section will be devoted to a review of results which have been obtained from the EW-scale ν_R model [6,7]. Since the previous section and the one that follows are necessary to introduce the model to readers who are not familiar with the model and, in particular, its phenomenological consequences, we include similar reviews in all related papers.

III. ELECTROWEAK PRECISION CONSTRAINTS ON THE EW ν_R MODEL [6]

The presence of mirror quark and lepton $SU(2)$ doublets can, by themselves, seriously affect the constraints coming from electroweak precision data. As noticed in Ref. [3], the positive contribution to the S parameter coming from the extra right-handed mirror quark and lepton doublets could be partially canceled by the negative contribution coming from the triplet Higgs fields. Reference [6] has carried out a detailed analysis of the electroweak precision parameters S and T and found that there is a large parameter space in the model which satisfies the present constraints and that there is *no fine-tuning* due to the large size of the allowed parameter space. It is beyond the scope of this paper to show more details here, but a representative plot would be helpful. Figure 1 shows the contribution of the scalar sector versus that of the mirror fermions to the S parameter within 1σ and 2σ. In the above plot, Ref. [6] took, for illustrative purposes, 3500 data points that fall inside the 2σ region with about 100 points falling inside the 1σ region. More details can be found in Ref. [6].

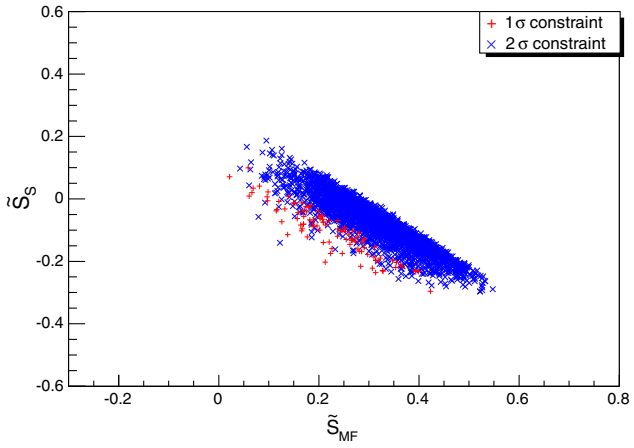

FIG. 1. The plot shows the contribution to the S parameter for the scalar sector ($\tilde{S}_S$) vs the mirror fermion sector ($\tilde{S}_{MF}$) within the 1σ and 2σ allowed regions. The negative contribution to the S parameter from the scalar sector tends to partially cancel the positive contribution from the mirror fermion sector, and the total sum of the two contributions agrees with experimental constraints.

IV. REVIEW OF THE SCALAR SECTOR OF THE EW ν_R MODEL IN LIGHT OF THE DISCOVERY OF THE 125 GEV SM-LIKE SCALAR

In light of the discovery of the 125 GeV SM-like scalar [7], it is imperative that any model beyond the SM (BSM) show a scalar spectrum that contains at least one Higgs field with the desired properties as required by experiment. The present data from CMS and ATLAS only show signal strengths that are compatible with the SM Higgs boson. The definition of a signal strength μ is as follows:

$$\sigma(H\text{-decay}) = \sigma(H\text{-production}) \times BR(H\text{-decay}) \quad (4)$$

and

$$\mu(H\text{-decay}) = \frac{\sigma(H\text{-decay})}{\sigma_{\rm SM}(H\text{-decay})}. \quad (5)$$

To really distinguish the SM Higgs field from its impostor, it is necessary to measure the partial decay widths and the various branching ratios. In the present absence of such quantities, the best one can do is to present cases which are consistent with the experimental signal strengths. This is what was carried out in Ref. [7].

The minimization of the potential containing the scalars shown above breaks its global symmetry $SU(2)_L \times SU(2)_R$ down to a custodial symmetry $SU(2)_D$ which guarantees at tree level $\rho = M_W^2/M_Z^2\cos^2\theta_W = 1$ [7]. The physical scalars can be grouped, based on their transformation properties under $SU(2)_D$, as follows:

$$\begin{aligned}
\text{five-plet(quintet)} &\to H_5^{\pm\pm}, H_5^{\pm}, H_5^0, \\
\text{triplet} &\to H_3^{\pm}, H_3^0, \\
\text{triplet} &\to H_{3M}^{\pm}, H_{3M}^0, \\
\text{three singlets} &\to H_1^0, H_{1M}^0, H_1^{0\prime}, \quad (6)
\end{aligned}$$

The three custodial singlets are the CP-even states, one combination of which can be the 125 GeV scalar. In terms of the original fields, one has $H_1^0 = \phi_2^{0r}$, $H_{1M}^0 = \phi_{2M}^{0r}$, and $H_1^{0\prime} = \frac{1}{\sqrt{3}}(\sqrt{2}\chi^{0r} + \xi^0)$. These states mix through a mass matrix obtained from the potential, and the mass eigenstates are denoted by $\tilde{H}$, $\tilde{H}'$, and $\tilde{H}''$, with the convention that the lightest of the three is denoted by $\tilde{H}$, the next heavier one by $\tilde{H}'$, and the heaviest state by $\tilde{H}''$.

To compute the signal strengths μ, Ref. [7] considers $\tilde{H} \to ZZ, W^+W^-, \gamma\gamma, b\bar{b}, \tau\bar{\tau}$. In addition, the cross section of $gg \to \tilde{H}$ related to $\tilde{H} \to gg$ was also calculated. A scan over the parameter space of the model yielded *two interesting scenarios* for the 125 GeV scalar: 1) *Dr. Jekyll*'s scenario in which $\tilde{H} \sim H_1^0$, meaning that the SM-like component $H_1^0 = \phi_2^{0r}$ is *dominant*; and 2) *Mr. Hyde*'s scenario in which $\tilde{H} \sim H_1^{0\prime}$, meaning that the SM-like component $H_1^0 = \phi_2^{0r}$ is *subdominant*. Both scenarios give signal strengths compatible with experimental data, as shown in Fig. 2.

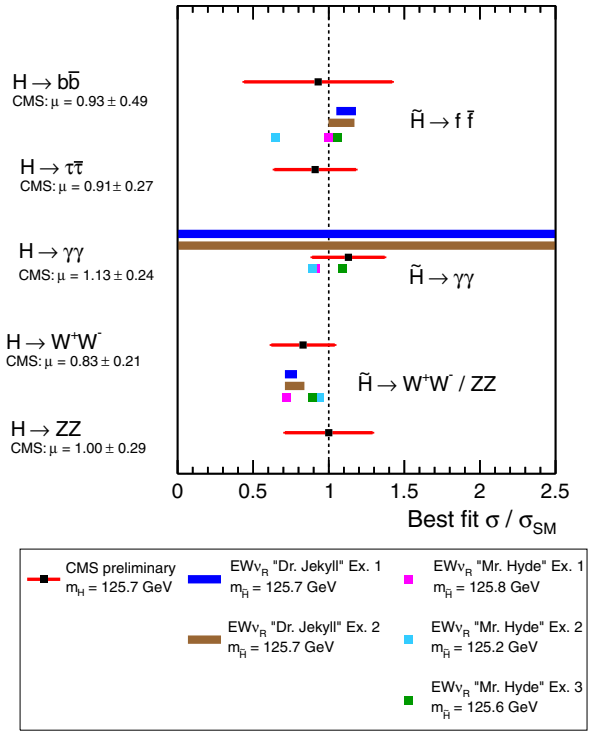

FIG. 2. The predictions of $\mu(\tilde{H} \to b\bar{b}, \tau\bar{\tau}, \gamma\gamma, W^+W^-, ZZ)$ in the EW ν_R model for examples 1 and 2 in the *Dr. Jekyll* scenario and examples 1, 2, and 3 in the *Mr. Hyde* scenario as discussed in Ref. [7], in comparison with corresponding best-fit values by CMS [14–17].

As we can see from Fig. 2, both the SM-like scenario (*Dr. Jekyll*) and the *more interesting scenario* which is very unlike the SM (*Mr. Hyde*) agree with experiment. As stressed in Ref. [7], present data cannot tell whether or not the 125 GeV scalar is truly SM-like or even if it has a dominant SM-like component. It has also been stressed in Ref. [7] that it is essential to measure the partial decay widths of the 125 GeV scalar to truly reveal its nature. Last but not least, in both scenarios, $H^0_{1M} = \phi^{0r}_{2M}$ is subdominant but is essential to obtain the agreement with the data as shown in Ref. [7].

As discussed in detail in Ref. [7], for proper vacuum alignment, the potential contains a term proportional to λ_5 [Eq. (32) of Ref. [7]], and it is this term that prevents the appearance of Nambu-Goldstone (NG) bosons in the model. The would-be NG bosons acquire a mass proportional to λ_5.

An analysis of CP-odd scalar states H^0_3, H^0_{3M} and the heavy CP-even states $\tilde{H}'$, and $\tilde{H}''$ was presented in Ref. [7]. The phenomenology of charged scalars including the doubly charged ones was also discussed in Ref. [9].

The phenomenology of mirror quarks and leptons was briefly discussed in Ref. [3] and a detailed analysis of mirror quarks will be presented in this paper. It suffices to mention here that mirror fermions decay into SM fermions through the process $q^M \to q\phi_S$, $l^M \to l\phi_S$, with ϕ_S "appearing" as missing energy in the detector. Furthermore, the decay of mirror fermions into SM ones can happen outside the beam pipe and inside the silicon vertex detector. Searches for non-SM fermions do not apply in this case. It is beyond the scope of the paper to discuss these details here.

V. YUKAWA INTERACTIONS BETWEEN MIRROR AND SM QUARKS

(1) *The interactions:*

The EW ν_R model has been extended to include an investigation of neutrino and charged lepton mass matrices and mixings [8]. In Ref. [8], a non-Abelian discrete symmetry group A_4 was assumed and was applied to the Higgs singlet sector which is responsible for the Dirac masses of the neutrinos. Following Ref. [8], we list the assignments of the SM and mirror fermions, as well as those for the scalars under A_4. From this assignment, one obtains the following Yukawa interactions in terms of quark mass eigenstates [$q^d_L = (d_L, s_L, b_L)$, $q^u_L = (u_L, c_L, t_L)$, $q^{M,d}_R = (d^M_R, s^M_R, b^M_R)$, $q^{M,u}_R = (u^M_R, c^M_R, t^M_R)$]:

$$L_S = \bar{q}^d_L U^{d\dagger}_L M^d_\phi U^{d^M}_R q^{M,d}_R + \text{H.c.} = \bar{q}^d_L \bar{M}^d_\phi q^{M,d}_R + \text{H.c.} \quad (7)$$

for the down-quark sector, and

$$L_S = \bar{q}^u_L U^{u\dagger}_L M^u_\phi U^{u^M}_R q^{M,u}_R + \text{H.c.} = \bar{q}^u_L \bar{M}^u_\phi q^{M,u}_R + \text{H.c.} \quad (8)$$

for the up-quark sector, and where

$$M^{d,u}_\phi = \begin{pmatrix} g^{d,u}_{0S}\phi_{0S} & g^{d,u}_{1S}\phi_{3S} & g^{d,u}_{2S}\phi_{2S} \\ g^{d,u}_{2S}\phi_{3S} & g^{d,u}_{0S}\phi_{0S} & g^{d,u}_{1S}\phi_{1S} \\ g^{d,u}_{1S}\phi_{2S} & g^{d,u}_{2S}\phi_{1S} & g^{d,u}_{0S}\phi_{0S} \end{pmatrix}. \quad (9)$$

The mixing parameters involved in the decay $q^{M,i}_R \to q^j_L + \phi_l$, where i and j denote quark flavors and $l = 0, \ldots, 3$, are contained in the parametrizations of $\bar{M}^{d,u}_\phi$ as well as in Eq. (9).

An important remark is in order here. Unlike the Yukawa couplings g_{Sl} of the lepton sector, which are constrained by rare processes such as $\mu \to e\gamma$, no such constraint exists for $g^{d,u}_{iS}$, and they can be arbitrarily small, as the present upper bounds on $\text{BR}(t \to qZ)$ from CMS and ATLAS are 5×10^{-4} and 7×10^{-4}, respectively, and are not "low" enough to constrain the Yukawa couplings g_{Sq}. This can give rise to displaced vertices of the type shown in Fig. 3. This kind of rare decay mode ($t \to qZ$, etc.) should exist through a loop diagram as do the ones calculated in Ref. [13] for $\mu \to e\gamma$. These processes are indeed under investigation by the authors of Ref. [13], and the results indicate values for BR which are many orders of magnitudes smaller than the current limits even when $g_{Sq} \sim O(1)$.

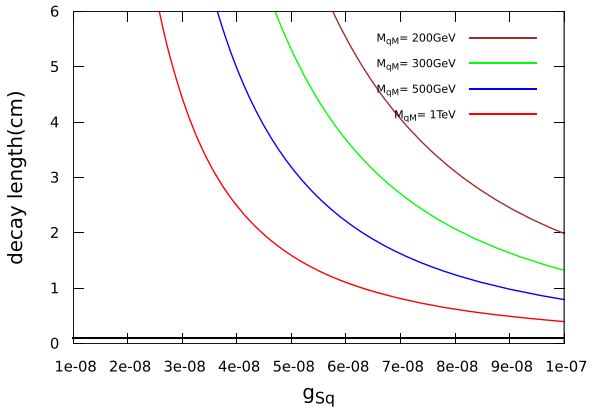

FIG. 3. Variation of the decay length (cm) with the generic coupling g_{Sq} varying in the range from 10^{-8} to 10^{-7} for four different values of the mirror quark masses ($M_{q^M} = 200$, 300, 500, and 1000 GeV). The black horizontal line in the plot corresponds to the decay length of 1 mm. So any macroscopic decay length of the mirror quarks above the black line is significantly different from the decay length coming from the bottom quarks' displaced vertices.

(2) *The decay width:*

Since we will be concentrating below on the production and signature of the lightest mirror quark, the decay mode that is allowed is $q^M \to q\phi_S$ or $b\phi_S$. As stressed in Ref. [3], the singlet scalars are assumed to be much lighter than the quarks (both SM and mirror), and we will neglect their masses in the computation of the decay width. One obtains

$$\Gamma(q^M \to q + \phi^\star) = \frac{g_{Sq}^2}{64\pi} m_{q^M} \left(1 - \frac{m_q^2}{m_{q^M}^2}\right) \times \left(1 + \frac{m_q}{m_{q^M}} - \frac{m_q^2}{2m_{q^M}^2}\right), \quad (10)$$

where explicit expressions for the generic coupling g_{Sq} in Eq. (10) can be obtained by using Eqs. (7), (8), and (9). In g_{Sq}, one finds the Yukawa coupling and various mixing angles. Since the decay length is $\gamma\beta\hbar c/\Gamma(q^M \to q + \phi^\star)$, one easily imagine that it can be *macroscopic*; i.e. > 1 mm if g_{Sq} is sufficiently small. In Fig. 3 the variation of the decay length (cm) with the generic coupling g_{Sq} varying in between 10^{-8} and 10^{-7} is shown. For these values of the coupling g_{Sq}, the decays of these lightest mirror quarks can produce displaced vertices with decay length varying in the range of a few mm to a few cm, which can be easily distinguished from the displaced vertices produced by bottom quarks having an average decay length of ~0.5 mm. Such a macroscopic decay length can presently be missed due to the nature of the algorithms of the LHC detectors CMS and ATLAS.

VI. PHENOMENOLOGY: NEW PHYSICS AT THE LHC

In this section, we will discuss the collider signature of this model in the context of the LHC experiment. The LHC is a proton-proton collider. Therefore, the strongly interacting particles are copiously produced (if kinematically accessible). In this work, we have studied the production and signature of mirror quarks. Mirror quarks are pair-produced at the LHC, and pair production takes place via gauge interaction only. At the partonic level, the $gg \to q^M\bar{q}^M$ process is mediated by a gluon in the s channel or a mirror quark in the t channel, whereas the $q\bar{q} \to q^M\bar{q}^M$ process is only mediated by a gluon in the s channel. While the electroweak diagrams also contribute to $q\bar{q} \to q^M\bar{q}^M$, these contributions are suppressed by a relative factor of $(\alpha_{\rm EW}/\alpha_s)^2$. Given that they do not bring in any new topologies, their contributions are subdominant. Due to a larger production cross section, we have studied the production and signature of the lightest mirror quark. Being the lightest, it can only decay into a SM quark (light quark or b quark) and the singlet scalar ϕ_S: $q^M \to q\phi_S$ or $b\phi_S$. Here, we have assumed that the d^M is the lightest mirror quark, making the decay products $b\phi_S$ or $(s, d)\phi_S$.

These decays take place via Yukawa interactions. Since these Yukawa couplings are a free parameter in this model, the decay branching ratios of a mirror quark into a light quark or a b quark are arbitrary. Therefore, the pair production of the lightest mirror quark at the LHC gives rise to two high transverse momentum jets (light quark jets or b jets) in association with large missing transverse energy ($\not{p}_T$):

$$pp \to q^M\bar{q}^M \to q\bar{q} + \not{p}_T \quad \text{or} \quad b\bar{b} + \not{p}_T. \quad (11)$$

The missing transverse momentum arises from the very light singlet scalars ϕ_S which remain invisible in the detector. Before going into the analysis of signal and background in the context of LHC run II with a 13 TeV center-of-mass energy, it is important to discuss LHC 8 TeV bounds on this model. There is no dedicated study available from the ATLAS or CMS collaborations in the context of the present model. However, the main signatures of this model, namely jets $+ \not{p}_T$ or $2b + \not{p}_T$, have already been studied by the ATLAS [18] and CMS [19,20] collaborations in the context of supersymmetry. The analysis of the CMS Collaboration [19] is based on the data collected by the CMS detector in proton-proton collision at $\sqrt{s} = 8$ TeV with an integrated luminosity of 11.7 fb^{-1}. The observed jets $+ \not{p}_T$ or $2b + \not{p}_T$ data are consistent with the SM background prediction. The absence of any excess of such events was then translated to an upper bound on the production cross section times branching ratio of any beyond-SM process which gives rise to a similar signature. In our analysis, we have used the bounds from Ref. [19] to impose constraints on the mirror quark mass and branching ratios to light jets and b jets. In Fig. 4, we have presented (the black lines) 95% C.L. upper limits on the theory production cross section times branching ratio into jets $+ \not{p}_T$ (left panel) and b-jets $+ \not{p}_T$ (right panel) obtained by the CMS group [19] with 8 TeV center-of-mass energy and 11.7 fb^{-1} integrated luminosity. Figure 4 also shows our model prediction for the production cross section times branching ratio for different values of the branching ratio. Figure 4 (left panel) shows that for a large $q_M \to q\phi_S$ branching ratio, a mirror quark mass below about 600 GeV is excluded, whereas, if the branching ratio of mirror quark into a light quark is below 50%, then there is no bound on the mirror quark mass. Similarly, if the branching ratio of $q_M \to b\phi_S$ is small, then there is no bound from Ref. [19]. It is important to note that these bounds are only applicable when mirror quarks decay at the hard scattering point, i.e., only for large decay widths of the mirror quarks. However, as discussed in the previous

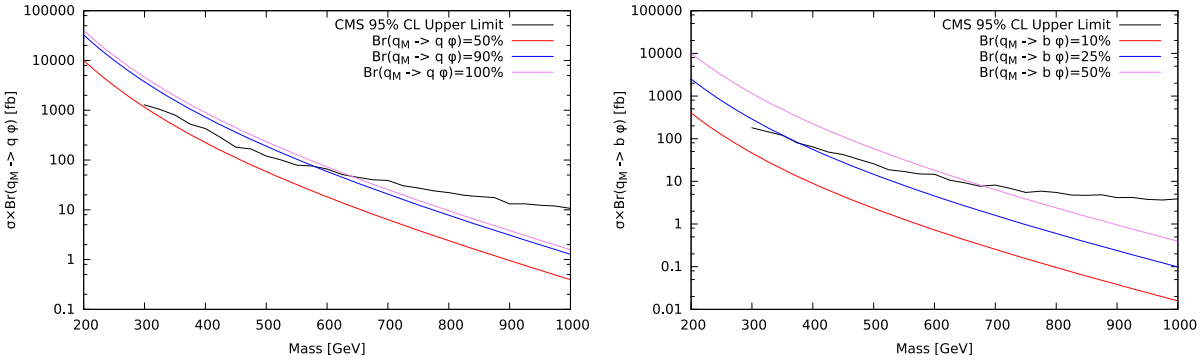

FIG. 4. Black line corresponds to 95% C.L. upper limits on the theory production cross section times branching ratio into jets + $\not{p}_T$ (left panel) and b-jets + $\not{p}_T$ (right panel) obtained by the CMS group [19] with 8 TeV center-of-mass energy and 11.7 fb^{-1} integrated luminosity. Other lines corresponds to our model prediction for the production cross section times branching ratio for different values of the branching ratio.

section, in the context of this model, the mirror quark decay width could be small enough for the hadronization of the mirror quarks and displaced decay of the hadronized mirror quarks. Such an event is not reconstructed by the present LHC multijet search algorithm and can be missed. In this case, the above lower bounds on mirror quark masses are not applicable.

After discussing the LHC 8 TeV bounds on the mirror quark mass, we are now equipped to discuss the phenomenology of this model in the context of LHC run II with 13 TeV center-of-mass energy.

Several SM processes constitute potential backgrounds for the signal of Eq. (11), and we now discuss the dominant ones in succession:

(1) An irreducible background arises from the production of a Z boson in association with multiple jets. The Z boson decays invisibly and gives rise to the missing transverse energy signature

$$pp \to Z + n\text{-jets} \to \nu\bar{\nu} + n\text{-jets}. \qquad (12)$$

We use the ALPGEN [21] generator to estimate the Z + jets (up to 3-jets) background contribution. Although the total cross section for this process is very large, the imposition of sufficiently strong p_T and rapidity requirements on the jets serves to suppress it strongly. It is important to note that our analysis will not be very sophisticated; it is quite conceivable that we might underestimate the background, especially where jet reconstruction is concerned.

(2) The production of $W^{\pm}$ in association with multiple jets (up to 3-jets) can also be a possible source of background if the $W^{\pm}$ decays leptonically and the charged lepton is missed somehow. To be specific, we consider the leptons to be undetectable if it either falls outside the rapidity coverage ($|\eta| \geq 2.5$), or if it is too soft ($p_T \leq 20$ GeV), or if it lies too close to any of the jets. In this case, the neutrino and the missing lepton together give rise to the missing transverse momentum. We also estimate this background using ALPGEN. Given the fact that the W has a substantial mass and that it is produced with relatively low rapidity, it stands to reason that the charged lepton would, most often, be well within the detector and also have sufficient p_T to be detectable. Consequently, the probability of missing the charged lepton is small, and this background would be suppressed considerably.

(3) Significant background contribution can come from the production of multiple jets: $pp \to nj$. In this case, there is no real source of missing transverse momentum. However, mismeasurement of the p_T of jets can lead to some amount of missing transverse momentum. Since the cross section for the aforementioned process is huge, this process, in principle, could contribute significantly to the background. In this case also, we have used ALPGEN to compute the multijets (up to 6-jets) background.

(4) The production of $t\bar{t}$ pairs in association with a W or Z boson (W or Z) followed by the leptonic decay of the W or invisible decay of the Z also gives rise to a jets + $\not{E}_T$ background. In this case, neutrinos in the decay of W or Z give rise to the missing energy. The production of $t\bar{t} + Z/W$ contributes significantly to the jets + $\not{E}_T$ background for higher jet multiplicity, since hadronic decay of $t\bar{t}$ gives rise to 6-jets at parton level. In fact, $t\bar{t} + Z/W$ is the dominant background for a jets + $\not{E}_T$ signature for jet multiplicity greater than 4 (see Table 5 of Ref. [18]). However, for low jet multiplicity, W/Z + jets is the dominant background for a jets + $\not{E}_T$ signature after selection cuts are introduced. For example, if we consider events with at least 2-jets + $\not{E}_T$ (which is the signal under consideration in this paper), the W/Z + jets contribution is at least 10 times bigger than the $t\bar{t} + Z/W$ contribution [18].

At this stage, we are equipped to develop a systematic methodology of suppressing the SM backgrounds without drastically reducing the signal. A fruitful perusal of such a methodology requires that we carefully examine and compare the phase space distributions of different kinematic variables for the signal as well as the backgrounds discussed above. However, before we embark on the mission to suppress the aforementioned backgrounds, it is important to list a set of basic requirements for jets to be visible at the detector. It should be noted that any realistic detector has only a finite resolution; this applies to energy/transverse momentum measurements as well as the determination of the angle of motion. For our purpose, the latter effect can be safely neglected, and we simulate the former by smearing the energy with Gaussian functions:

$$\frac{\Delta E}{E} = \frac{a}{\sqrt{E/\mathrm{GeV}}} \oplus b, \tag{13}$$

where $a = 100\%$, $b = 5\%$, and $\oplus$ denotes a sum in quadrature [22]. Keeping in mind the LHC environment as well as the detector configurations, we demand that, to be visible, a jet must have an adequately large transverse momentum and be well inside the rapidity coverage of the detector—namely,

$$p_T^j > 40 \text{ GeV}, \tag{14}$$

$$|\eta_j| \leq 2.5. \tag{15}$$

We demand that jets be well separated so that they can be identified as individual entities. To this end, we use the well-known cone algorithm defined in terms of a cone angle $\Delta R_{ij} \equiv \sqrt{(\Delta\phi_{ij})^2 + (\Delta\eta_{ij})^2}$, with $\Delta\phi$ and $\Delta\eta$ being the azimuthal angular separation and rapidity difference between two particles. Quantitatively, we impose

$$\Delta R_{jj} > 0.7. \tag{16}$$

Furthermore, the event must be characterized by a minimum missing transverse momentum defined in terms of the total visible momentum—namely,

$$\not{p}_T \equiv \sqrt{\left(\sum_{\text{vis}} p_x\right)^2 + \left(\sum_{\text{vis}} p_y\right)^2} > 20 \text{ GeV}. \tag{17}$$

It has been discussed already that for some of the SM backgrounds, the hard (parton level) process does not even have a source of missing energy. However, the multijet final state could potentially be associated with a missing transverse momentum only on account of mismeasurements of the jet energies. A minimum requirement of the missing transverse momentum keeps these backgrounds well under control. The requirements summarized in Eqs. (14)–(17) constitute our *acceptance cuts*.

With the set of acceptance cuts and detector resolution defined in the previous paragraph, we compute the signal and background cross sections at the LHC operating with $\sqrt{s} = 13$ TeV and display them in Table II. Clearly, the backgrounds are very large compared to the signal. The dominant SM background contribution arises from multijets. In order to enhance the signal-to-background ratio, we study distributions of different kinematic observables. In Fig. 5, we display the p_T distributions of the signal and background jets after ordering them according to their p_T ($p_T^{j_1} > p_T^{j_2}$). The left panel corresponds to the hardest jet, and the right panel corresponds to the second hardest jet. From the shape of the p_T distributions in Fig. 5, it is obvious that any harder p_T cut on jets will simultaneously reduce signal as well as background. In Fig. 6, we display the missing transverse momentum distribution (left panel) and effective mass distribution (right panel) for the signal and background. The effective mass is defined as the scalar sum of the transverse momenta of all the visible particles (in this case all jets with $p_T > 40$ GeV), as well as the total missing transverse momentum. It can be expressed, in our case, through

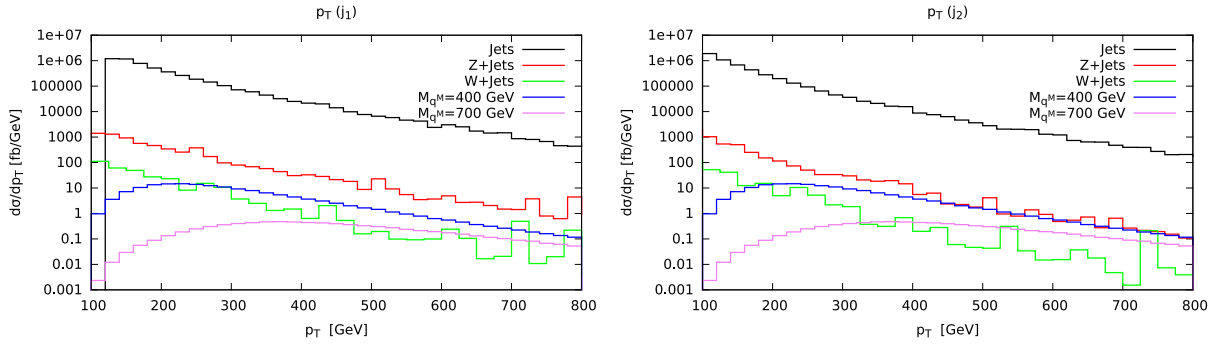

FIG. 5. Transverse momentum distributions of jets (left panel: hardest jet; right panel: second hardest jet) after ordering them according to their p_T hardness [$p_T(j_1) > p_T(j_2)$] for signal and background. We have assumed a 13 TeV center-of-mass energy for the proton-proton collision.

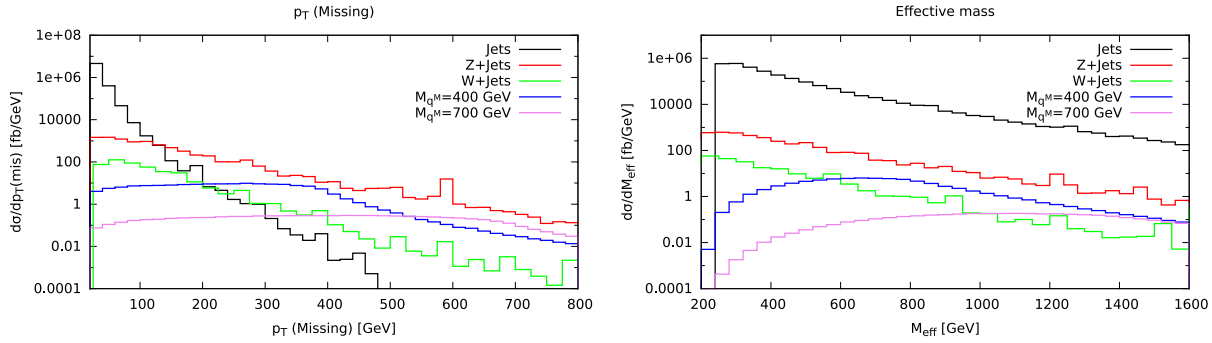

FIG. 6. Missing transverse momentum (left panel) and effective mass (right panel) distributions for signal ($M = 400$ and 700 GeV) and background (jets, $Z +$ jets, $W +$ jets).

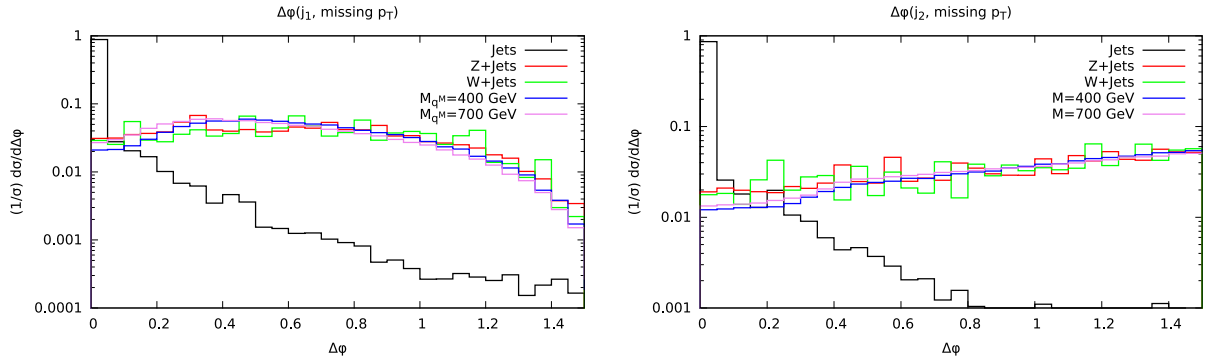

FIG. 7. Normalized $\Delta\phi(\text{jet}, \vec{\not{p}}_T)$ distribution for signal and background.

$$M_{\text{eff}} = \sum_j p_T^j + \not{p}_T. \tag{18}$$

The missing transverse momentum distribution in the left panel of Fig. 6 shows that the multijet background is peaked at a relatively low $\not{p}_T$. Since, for this process, a missing transverse momentum can arise only from mismeasurement, this contribution can be suppressed significantly by introducing a harder $\not{p}_T$ cut, whereas Fig. 6 (right panel) shows that a harder M_{eff} cut helps to reduce the $Z/W +$ jets background. In Fig. 7, we present the normalized azimuthal angular distribution between the hardest jet and $\vec{\not{p}}_T$ [$\Delta\phi(j_1, \vec{\not{p}}_T)$: left panel] and the second hardest jet and $\vec{\not{p}}_T$ [$(\Delta\phi(j_2, \vec{\not{p}}_T)$: right panel]. Fig. 7 shows that lower bounds on $\Delta\phi(j_1, \vec{\not{p}}_T)$ and $\Delta\phi(j_2, \vec{\not{p}}_T)$ clearly reduce the multijet background. Finally, we consider the ratio $\not{p}_T/M_{\text{eff}}$, and in Fig. 8, present the distributions in the same. The background peaks around $\not{p}_T/M_{\text{eff}} \sim 0.1$, and it is obvious that it would be reduced significantly if a lower bound on this ratio is imposed. In view of the characteristic distributions presented in Figs. 5 to 8, we summarize our final event selection criteria in Table III. In Table IV, we summarize the signal and the SM background cross sections after the imposition of the selection cuts listed in Table III.

In order to calculate the discovery reach of the LHC with 13 TeV center-of-mass energy, we define the signal to be observable for a integrated luminosity $\mathcal{L}$ if

(1)

$$\frac{N_S}{\sqrt{N_B + N_S}} \geq 5 \quad \text{for } 0 < N_B \leq 5N_S, \tag{19}$$

where $N_{S(B)} = \sigma_{S(B)}\mathcal{L}$ is the number of signal (background) events for an integrated luminosity $\mathcal{L}$.

(2) For zero background events, the signal is observable if there are at least five signal events.

(3) In order to establish the discovery of a small signal (which could be statistically significant, i.e. $N_S/\sqrt{N_B} \geq 5$) on top of a large background, we

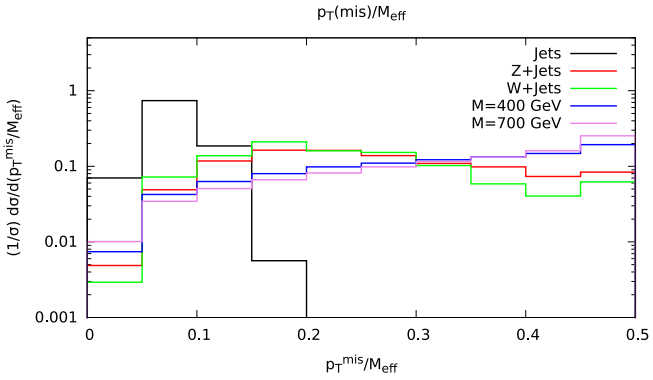

FIG. 8. Normalized $\not{p}_T/M_{\text{eff}}$ distribution for signal and background.

TABLE I. A_4 assignments for leptons and Higgs fields.

Field	$(\nu, l)_L$	$(\nu, l^M)_R$	e_R	e_L^M	ϕ_{0S}	$\tilde{\phi}_S$	Φ_2
A_4	$\underline{3}$	$\underline{3}$	$\underline{3}$	$\underline{3}$	$\underline{1}$	$\underline{3}$	$\underline{1}$

TABLE II. Signal and SM background cross sections (in fb) after the acceptance cuts. We have also estimated the $t\bar{t}Z$ background using the ALPGEN generator. Assuming invisible decay of the Z boson, the $t\bar{t}Z$ cross-section is estimated to be about 100 fb at the LHC with 13 TeV center-of-mass energy. The other background contributions are orders of magnitude larger than the $t\bar{t}Z$ contribution. As a result, we have not included the $t\bar{t}Z$ contribution in this table.

Cross section in fb					
Signal		Background			
M_{q^M}	[GeV]	Jets	$Z+$jets	$W+$jets	Total
400	700				
3.1×10^3	165.3	1.01×10^8	1.56×10^5	1.05×10^4	1.01×10^8

TABLE III. Selection cuts.

Variable	Lower bound	Upper bound
$\not{p}_T$	160 GeV	
$p_T(j_1)$	130 GeV	
$p_T(j_2)$	60 GeV	
η_j	−2.5	2.5
$\Delta R_{j_1 j_2}$	0.7	
$\Delta\phi(j, \vec{\not{p}}_T)$	0.4	
M_{eff}	1000 GeV	
$\not{p}_T/M_{\text{eff}}$	0.2	

TABLE IV. Signal and SM background cross sections (in fb) after the selection cuts.

Cross section in fb				
Signal		Background		
M_{q^M}	[GeV]	Jets	$Z/W+$jets	Total
400	700			
111.6	51.8	⋯	400	400

need to know the background with exquisite precision. However, such precise determination of the SM background is beyond the scope of this present article. Therefore, we impose the requirement $N_B \leq 5N_S$ to avoid such possibilities.

The branching ratio of $q^M \to q\phi_s$ is a free parameter in this model. Therefore, in Fig. 9, we have presented the required integrated luminosity for the discovery of mirror quark as a function of the branching ratio $(q^M \to q\phi_S)$ for two different values of mirror quark mass. In Fig. 10, the required integrated luminosity (color gradient) for 5σ discovery at the LHC with 13 TeV center-of-mass energy is presented as a function of both the mirror quark mass (along the x axis) and the branching ratio $q^M \to q\phi_S$ (along the y axis).

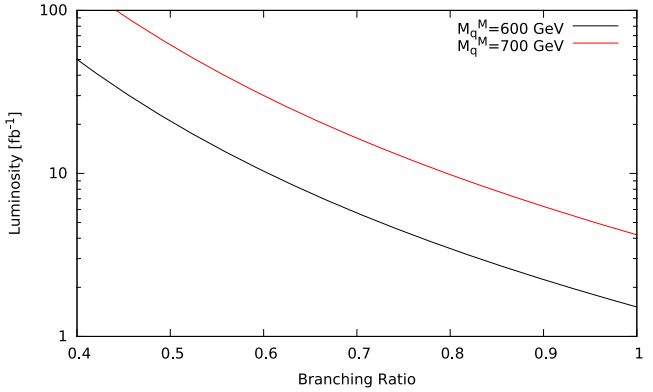

FIG. 9. Required integrated luminosity for 5σ discovery at the LHC with 13 TeV center-of-mass energy as a function of the branching ratio $(q^M \to q\phi_S)$ for two different values of mirror quark masses (400 and 700 GeV).

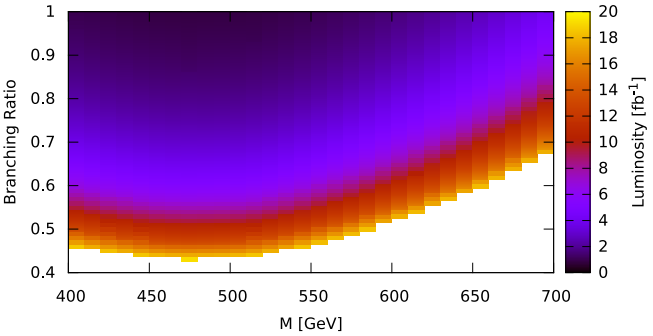

FIG. 10. The required integrated luminosity (color gradient) for 5σ discovery at the LHC with 13 TeV center-of-mass energy is presented as a function of the mirror quark mass (along the x axis) and the branching ratio $q^M \to q\phi_S$ (along the y axis).

In this section, we have discussed the production and signature of the lightest mirror quark. This analysis is based on the assumption of prompt decays of the mirror quarks. In the framework of this model, the lightest mirror quark decays into a SM quark and ϕ_S with a Yukawa coupling which is a free parameter. Small values of this Yukawa coupling result in small decay widths, and hence a long lifetime for the lightest mirror quark. In this case, the produced mirror quarks hadronize before they decay. Depending on the smallness of the Yukawa coupling, the hadronized mirror quarks decay a few mm to a few cm away from the hard scattering point. The decay of a mirror quark gives rise to a missing particle and a jet. However, if the decays take place at a point different from the primary vertex, then present LHC jet reconstruction algorithms categorize the resulting jets as "fake jets"

[10,11]. The LHC jet reconstruction algorithm is designed to distinguish between jets produced in proton-proton collisions and "fake jets" not originating from hard scattering events. "Fake jets" come from different sources like the collision of one proton of the beam with the residual gas within the beam pipe, beam-halo events, cosmic rays, etc. The LHC jet reconstruction algorithm employs criteria like the distribution of energy deposits by the jet, the shower shape and its direction, and in particular the pointing to the interaction point to discriminate between collision jets and "fake jets." In the context of our model, if the mirror quark decays away from the interaction point, then the resulting jets will not point towards the interaction point, and hence will be considered "fake jets" by the present LHC jet reconstruction algorithm. Moreover, in the absence of any information about the other decay product—namely, the invisible scalar ϕ_S—it will be very challenging to reconstruct the secondary vertex. Therefore, in order to study such events, a new algorithm for the jet reconstruction is required. It is beyond the scope of our parton-level Monte Carlo analysis to study such events.

VII. CONCLUSION

We have explored the new physics possibilities at the 13 TeV LHC run. The model used is well motivated, and was proposed to obtain tiny neutrino masses via the seesaw mechanism with the RH neutrino at the EW scale. The gauge symmetry is $SU(2)_w \times U(1)_Y$, but the fermion as well as the Higgs sector is extended. For the fermions, we have both the left- and right-handed doublets, as well as singlets under the $SU(2)_W$ gauge symmetry. In this model the RH quark/lepton doublets and the left-handed singlets are called mirror quarks and leptons. The scalar sector of the original EW-scale ν_R model contains two triplets, one doublet, and one singlet. However, the extended EW-scale ν_R model contains two triplets, two doublets (one coupled to the SM fermions and the other to mirror fermions), and four singlets to accommodate the 125 GeV scalar and to discuss leptonic mixings. The model is derived using the above gauge symmetry, additional global symmetries, and discrete A_4 symmetry. As shown in the previous works, the model satisfies the EW precision constraints as well as the constraints from the 125 GeV Higgs data.

In this work, we have explored the implications of the model for the 8 and 13 TeV LHC. Since the model has colored quarks of chirality opposite to that of the SM quarks (the mirror quarks) and there is only one symmetry-breaking scale—the usual EW scale ~250 GeV, which gives masses to these mirror quarks—they cannot be heavier than ~900 GeV from the unitarity of the Yukawa couplings. Thus, these mirror quarks will be copiously produced at the LHC. Once produced, in the model, they can decay to ordinary quarks and singlet Higgs. At the interaction point, if the corresponding Yukawa coupling is not tiny, the final states are two ordinary quarks, or two b quarks and large missing energy due to the escaping singlet Higgs. We have calculated the production cross sections times the branching ratios of the mirror quarks to the ordinary light quarks or the b quarks. The relative branching ratios to the ordinary light quarks or the b quarks are unknown in the model. So, we have calculated the cross section times branching ratios as a function of the mirror quark masses for several values of the branching ratios. Comparing these with the corresponding experimental limit plots produced by the CMS Collaboration at the 8 TeV LHC, we find that the mass of the lightest mirror quark as low as ~600 GeV is allowed for $\mathrm{Br}(q_M \to q\phi_S) = 100\%\%$. However, if the branching ratio of $q_M \to q\phi_S$ is 50% or less, then there is no bound from the LHC 8 TeV data. Furthermore, this bound applies only to prompt decays of mirror quarks. For displaced decays with decay lengths greater than 1 mm or so, this bound is no longer valid and the mirror quark mass can be lower. Assuming prompt decays of mirror quarks, we have also calculated the signal as well as the SM background at the 13 TeV LHC. We find that the signal for the final-state signature with a 5σ confidence level can be observed for the lightest mirror quark mass of ~700 GeV with an integrated luminosity ~100 fb^{-1}.

The model has another interesting feature. For very tiny Yukawa couplings, the decays of these mirror quarks can produce displaced vertices with decay length in the cm range or larger. These events characteristics are very different from the displaced vertices produced by b quarks for which the average decay length is ~0.5 mm. Such unusual events may have been thrown out in the usual experimental analyses. A suitable algorithm may need to be developed to look for such events.

ACKNOWLEDGMENTS

We are grateful to J. Haley, A. Khanov of the ATLAS Collaboration, and G. Landsberg of the CMS Collaboration for several valuable discussions. The work of S. C., K. G., and S. N. was supported in part by U.S. DOE Grant No. DE-SC0010108. V. H. and P. Q. H. were supported in part by U.S. DOE Grant No. DE-FG02-97ER41027 and in part (P. Q. H.) by the Pirrung Foundation. S. C. is supported by the Pirrung Foundation.

[1] S. Weinberg, Baryon and Lepton Nonconserving Processes, Phys. Rev. Lett. **43**, 1566 (1979).
[2] T. D. Lee and C.-N. Yang, Question of parity conservation in weak interactions, Phys. Rev. **104**, 254 (1956).
[3] P. Q. Hung, A model of electroweak-scale right-handed neutrino mass, Phys. Lett. B **649**, 275 (2007).
[4] J. C. Pati and A. Salam, Lepton number as the fourth color, Phys. Rev. D **10**, 275 (1974); **11**, 703 (1975); R. N. Mohapatra and J. C. Pati, A natural left-right symmetry, Phys. Rev. D **11**, 2558 (1975); G. Senjanovic and R. N. Mohapatra, Exact left-right symmetry and spontaneous violation of parity, Phys. Rev. D **12**, 1502 (1975); G. Senjanovic, Spontaneous breakdown of parity in a class of gauge theories, Nucl. Phys. **B153**, 334 (1979); S. Chakdar, K. Ghosh, S. Nandi, and S. K. Rai, Collider signatures of mirror fermions in the framework of a left-right mirror model, Phys. Rev. D **88**, 095005 (2013).
[5] V. Khachatryan *et al.* (CMS Collaboration), Search for heavy neutrinos and W bosons with right-handed couplings in proton-proton collisions at $\sqrt{s} = 8$ TeV, Eur. Phys. J. C **74**, 3149 (2014).
[6] V. Hoang, P. Q. Hung, and A. S. Kamat, Electroweak precision constraints on the electroweak-scale right-handed neutrino model, Nucl. Phys. **B877**, 190 (2013).
[7] V. Hoang, P. Q. Hung, and A. S. Kamat, Nonsterile electroweak-scale right-handed neutrinos and the dual nature of the 126 GeV scalar, Nucl. Phys. **B896**, 611 (2015).
[8] P. Q. Hung and T. Le, On neutrino and charged lepton masses and mixings: A view from the electroweak-scale right-handed neutrino model, J. High Energy Phys. 09 (2015) 001.
[9] A. Aranda, J. Hernandez-Sanchez, and P. Q. Hung, Implications of the discovery of a Higgs triplet on electroweak right-handed neutrinos, J. High Energy Phys. 11 (2008) 092.
[10] ATLAS Collaboration, Reports No. ATLAS-CONF-2012-020 and No. ATLAS-COM-CONF-2012-018.
[11] G. Aad *et al.* (ATLAS Collaboration), Characterisation and mitigation of beam-induced backgrounds observed in the ATLAS detector during the 2011 proton-proton run, J. Instrum. **8**, P07004 (2013).
[12] I. Montvay, Report No. DESY-87-147; A Chiral SU(2)-L x SU(2)-R gauge model on the lattice, Phys. Lett. B **199**, 89 (1987); Report No. DESY-87-077.
[13] P. Q. Hung, T. Le, V. Q. Tran, and T. C. Yuan, Lepton flavor violating radiative decays in EW-scale ν_R model: An update, J. High Energy Phys. 12 (2015) 169.
[14] S. Chatrchyan *et al.* (CMS Collaboration), Measurement of Higgs boson production and properties in the WW decay channel with leptonic final states, J. High Energy Phys. 01 (2014) 096.
[15] S. Chatrchyan *et al.* (CMS Collaboration), Measurement of the properties of a Higgs boson in the four-lepton final state, Phys. Rev. D **89**, 092007 (2014).
[16] S. Chatrchyan *et al.* (CMS Collaboration), Search for the standard model Higgs boson produced in association with a W or a Z boson and decaying to bottom quarks, Phys. Rev. D **89**, 012003 (2014).
[17] S. Chatrchyan *et al.* (CMS Collaboration), Evidence for the 125 GeV Higgs boson decaying to a pair of τ leptons, J. High Energy Phys. 05 (2014) 104.
[18] G. Aad *et al.* (ATLAS Collaboration), Search for squarks and gluinos with the ATLAS detector in final states with jets and missing transverse momentum using $\sqrt{s} = 8$ TeV proton-proton collision data, J. High Energy Phys. 09 (2014) 176.
[19] S. Chatrchyan *et al.* (CMS Collaboration), Search for supersymmetry in hadronic final states with missing transverse energy using the variables α_T and b-quark multiplicity in pp collisions at $\sqrt{s} = 8$ TeV, Eur. Phys. J. C **73**, 2568 (2013).
[20] V. Khachatryan *et al.* (CMS Collaboration), Searches for third-generation squark production in fully hadronic final states in proton-proton collisions at $\sqrt{s} = 8$ TeV, J. High Energy Phys. 06 (2015) 116.
[21] M. L. Mangano, M. Moretti, F. Piccinini, R. Pittau, and A. D. Polosa, ALPGEN, a generator for hard multiparton processes in hadronic collisions, J. High Energy Phys. 07 (2003) 001.
[22] G. Aad *et al.* (ATLAS Collaboration), Expected performance of the ATLAS experiment-Detector, trigger and physics, arXiv:0901.0512; G. L. Bayatian *et al.* (CMS Collaboration), CMS technical design report, Volume II: Physics performance, J. Phys. G **34**, 995 (2007).